Food and Bioprocess Technology (2023) 16:2016–2026
https://doi.org/10.1007/s11947-023-03050-z

RESEARCH

Improvement of Physicochemical and Antibacterial Properties of Nanoemulsified *Origanum vulgare* Essential Oil Through Optimization of Ultrasound Processing Variables

Bruno Dutra da Silva[1,2,3,5,7] · **Denes Kaic Alves do Rosário**[1,2,3,4,7] · **Yago Alves de Aguiar Bernardo**[1,2,3,5,6] · **Carlos Adam Conte-Junior**[1,2,3,5,6,7]

Received: 25 January 2023 / Accepted: 24 February 2023 / Published online: 4 March 2023

Abstract

Water solubility and increased specific surface area are some advantages that essential oil nanoemulsions have over pure oils. Numerous mechanisms to form nanoemulsions are reported in the literature, and even so, there are gaps in the correlations of processing variables and expected specific properties. This study applied a rotating core composite design (CCRD) to describe ultrasound processing variables on the physicochemical and antibacterial properties of *Origanum vulgare* essential oil nanoemulsion. Droplet size ranged from 41.67 to 231.83 nm with polydispersion between 0.21 and 0.46. All minimum inhibitory concentrations (MIC) observed in nanoemulsions (0.15–1.83 mg/mL) for *E. coli* and *S. aureus* were lower than in pure oil (2.36 mg/mL). Droplet size (41 nm), PDI (0.21), zeta potential (−10.13 mV), and MIC (≤ 0.23 mg/mL) properties could be obtained with optimized conditions of 2.9% Tween 80, 157 W, and 4.7 min sonication or 81.4 kJ/mL acoustic energy density. Optimized nanoemulsions stored at 4 °C showed stability over 30 days (< 150 nm), with growth kinetics of 2.54 nm/day. The effects observed in this study may solve some limitations of applying natural antimicrobials.

Keywords Sonication · Natural antimicrobials · Nanotechnology · Carvacrol · Outbreaks · Pathogens

Introduction

Delivery systems based on nanoemulsions have attracted attention in recent years in several research areas due to the droplet-improved properties, including the increased surface area of contact, protection of bioactive compounds, water solubility, and improved optical properties (McClements et al., 2021). Several authors consider nanoemulsions when the suspended droplets reach a diameter smaller than 200 nm (Donsi et al., 2016; Sharma et al., 2022). The selection of suitable technology for producing nanoemulsions with droplet sizes capable of improving the physicochemical properties of the system is crucial for possible commercial applications. Low-energy methods can prepare nanoemulsion through

✉ Denes Kaic Alves do Rosário
deneskaic@gmail.com

1 Analytical and Molecular Laboratorial Center (CLAn), Institute of Chemistry (IQ), Federal University of Rio de Janeiro (UFRJ), Cidade Universitária, 21941-909 Rio de Janeiro, RJ, Brazil

2 Center for Food Analysis (NAL), Technological Development Support Laboratory (LADETEC), Federal University of Rio de Janeiro (UFRJ), Cidade Universitária, 21941-598 Rio de Janeiro, RJ, Brazil

3 Laboratory of Advanced Analysis in Biochemistry and Molecular Biology (LAABBM), Department of Biochemistry, Federal University of Rio de Janeiro (UFRJ), Cidade Universitária, 21941-909 Rio de Janeiro, RJ, Brazil

4 Department of Food Engineering, Center for Agrarian Sciences and Engineering, Federal, University of Espírito Santo (UFES), Alto Universitário, 29500-000 S/N Guararema, Alegre, ES, Brazil

5 Graduate Program in Food Science (PPGCAL), Institute of Chemistry (IQ), Federal University of Rio de Janeiro (UFRJ), Cidade Universitária, 21941-909 Rio de Janeiro, RJ, Brazil

6 Graduate Program in Veterinary Hygiene (PPGHV), Faculty of Veterinary Medicine, Fluminense Federal University (UFF), Vital Brazil Filho, 24230-340 Niterói, RJ, Brazil

7 Nanotechnology Network, Carlos Chagas Filho Research Support Foundation of the State of Rio de Janeiro (FAPERJ), 20.020-000 Rio de Janeiro, RJ, Brazil

system phase inversion (phase inversion composition, phase inversion temperature, and emulsion inversion point) and high-energy methods through disruptive mechanical forces (homogenization high-pressure, microfluidization, high-shear, and ultrasound) (Galvão et al., 2018; Hasheminya & Dehghannya, 2022; Hien & Dao, 2021; Xu et al., 2020). The development of delivery systems for natural compounds based on nanoemulsions has been a trend observed in numerous studies published in recent years, with different techniques and different formulations (Sharma et al., 2022; Youssef et al., 2022). These studies are important to reinforce the area of knowledge about the improved physicochemical properties. However, the differences between the formulations hinder the standardization of the technique and the possibility of commercial application. In a previous study, da Silva et al. (2022b) suggested that the antibacterial activity of nanoemulsions is not only associated with the smaller droplet sizes but also with the surfactant:oil ratio (SOR), which should be ideal for maintaining the bioactive hydrophobic core. Thus, optimization studies are necessary for the development of nanoemulsions that not only focus on size reduction, but also enhance bioactivity for a given application.

The production of nanoemulsions by ultrasound has gained interest due to the low cost of implementation, energy efficiency, and control of process variables. The equipment's acoustic cavitations generate pressure fluctuations, collapsing microbubbles in the system. The collapse creates localized turbulence capable of causing the droplet to rupture, reducing its size (Bernardo et al., 2021). Final droplet properties such as size, polydispersity, zeta potential, and antibacterial activity can be influenced by processing parameters, including surfactant:oil ratio (SOR), surfactant type, sonication time, and ultrasound power (Teng et al., 2020). Several studies in recent years have produced essential oil nanoemulsions using ultrasound and obtaining significant variations in droplet size and polydispersity (Jiménez et al., 2018; Merghni et al., 2022). These factors are important when observing that some formulations fit the nanoemulsion classification, but the antibacterial effects are equal to or less than free essential oil (Ozogul et al., 2020).

The main limitation of essential oils for several applications is their insolubility in water, reducing the contact of bioactive compounds with bacterial cells in aqueous media. The improved properties of nanodroplets can increase the solubility of essential oils in aqueous media, and the increase in the specific surface area can favor the interaction of bioactive compounds of essential oils with bacterial cells (Araújo et al., 2018; Rosario et al., 2020). However, the standardization of processing variables for preparing *n*EO with improved properties is still poorly understood. Thus, this study aimed to optimize the *Origanum vulgare* essential oil nanoemulsion (*n*OEO) preparation to achieve improved physicochemical and antibacterial properties based on processing variables such as surfactant concentration, ultrasound power, and sonication time.

Material and Methods

Materials

The *Origanum vulgare* essential oil originated from Moldavia and was acquired from Ferquima Ltda. (São Paulo, Brazil). The oil was obtained by steam distillation, and the main constituents present were carvacrol (74%), *p*-cymene (5%), and thymol (2%), according to the manufacturer's technical report. The Tween 80 (HLB = 16) (Isofar, Brazil) used as a surfactant was purchased from Rei-Sol (Rio de Janeiro, Brazil). *Escherichia coli* ATCC 25,922 and *Staphylococcus aureus* ATCC 13,565 were obtained from the culture bank of Fundação Oswaldo Cruz (FIOCRUZ, Rio de Janeiro, Brazil).

Experimental Design

A central composite rotatable design (CCRD) was used in array 2^3, consisting of eight factorial points and six axial points with five repetitions at the central point (Table 1). Three independent variables were chosen, including surfactant concentration (X_1), ultrasound power (X_2), and sonication time (X_3). Droplet diameter (Y_1), polydispersity index (Y_2), zeta potential (Y_3), and minimum inhibitory concentration of *E. coli* and *S. aureus* (Y_4) were selected as response variables to determine the optimal conditions for processing the nanoemulsions. The experimental conditions of the central points were selected based on a meta-analysis study by da Silva et al. (2022b) on droplet sizes associated with antibacterial activity.

Nanoemulsion Preparation

Approximately 50 mL of a thick emulsion was prepared by fixed addition of 1% *Origanum vulgare* essential oil and variations in Tween 80 concentration based on CCRD. The remainder of the volume comprised ultrapure water (Mili-Q IQ 7005, Merck, Germany).

Table 1 Coding of independent variables according to the CCRD

	Levels				
Variables	−1.68	−1	0	+1	+1.68
SC (%)	0.31	1.0	2.0	3.0	3.68
UP (W)	21	35	55	75	89
ST (min)	1.59	5.0	10	15	18.40

SC surfactant concentration, *UP* ultrasound power, *ST* sonication time

The thick emulsion was prepared in Ultraturrax (IKA® T10, China) for 5 min at 10,000 rpm (^{Ø}stator: 10 mm/^{Ø}rotor: 7.6 mm). Subsequently, the emulsion was sonicated at different powers and sonication times in ultrasound (VCX-750 Ultrasonic Processor, 20 kHz, 750 W) with a 19 mm diameter probe (Sonics, Materials Inc., Newtown, USA). The effective power of the ultrasound was measured by calorimetry (Eq. 1), and the energy dissipated in the liquid was determined by the acoustic density energy (AED) (Eq. 2) (Ojha et al., 2018). To avoid the excessive rise in temperature generated by the sonication of the sample, the emulsion was cooled during processing using an ice bath (0 ± 1 °C). The temperature did not exceed 20 °C measured with the equipment's aid of a thermometer. After preparation, the nanoemulsions were stored at 4 °C until further tests were performed.

$$Effective\ power\ (W) = mC_p\left(\frac{\partial T}{\partial t}\right) \quad (1)$$

$$AED\ (\mathrm{kJ/mL}) = \frac{Effective\ power\ (W)\ \cdot\ processtime\ (s)}{Sample\ (mL)} \quad (2)$$

where m = mass of solvent (g), Cp = solvent specific heat (kJ/g), ∂T = increased temperature (°C), and ∂t = sonication time (s)

Droplet Size, Polydispersity Index (PDI), and Zeta Potential

The droplet diameter, PDI, and zeta potential of *n*OEO were determined in dynamic light scattering (Zetasizer LAB, Malvern Instruments, UK). The samples were diluted in deionized water in a proportion of 1 : 10, and the values were obtained by averaging three measurements at 25 °C. The refractive index selected was the average (1.490) of the refractive index of *Origanum vulgare* essential oil (1.508) and Tween 80 (1.473). Measurements were performed on the day of preparation.

Preparation of Bacterial Suspensions

E. coli ATCC 25,922 and *S. aureus* ATCC 13,565 were activated twice in brain heart infusion broth (Kasvi, Spain) with incubated at 37 °C for 24 h. After activation, *E. coli* was isolated on EMB agar (Kasvi, Spain), and *S. aureus* was isolated on Baird Parker agar supplemented with egg yolk tellurite (Kasvi, Spain), incubated at 37 °C for 24 h. Colonies of isolated bacteria were transferred to test tubes containing 5.0 mL of sterile saline solution at 0.85% (w/v). The turbidity was compared to a standard barium sulfate solution equivalent to the MacFarland 0.5 scale, corresponding to an approximate concentration of 8 log CFU/mL based on Clinical and Laboratory Standards Institute guidelines (CLSI, 2006).

Minimum Inhibitory Concentration (MIC)

The MIC for each bacteria was determined in a microdilution assay in sterile 96 U-bottom wells microplates (OLEN, China), based on the method described by (Wiegand et al., 2008). Final concentrations of 2.36, 1.18, 0.59, 0.29, 0.15, and 0.07 mg/mL were obtained from a stock solution with a concentration of 9.46 mg/mL diluted with sterile Mueller Hinton broth (Kasvi, Spain). One hundred microliters of *n*OEO and 100 µL of each bacterial suspension were added to each well to achieve approximately 5.5 log CFU/mL. Bacterial counts were confirmed on plate count agar at the time of testing. Microplates were incubated at 37 °C for 24 h, and MIC was considered the lowest concentration in preventing visible bacterial growth in microplate wells. Wells containing only Mueller Hinton broth and Mueller Hinton broth with bacterial inoculum was used for sterility and growth control, respectively. A solution containing *Origanum vulgare* essential oil + Mueller Hinton broth + Tween 80 (0.5%) at the same concentrations as the assay was used to evaluate the MIC of the non-nanoemulsified version.

Mathematical Modeling

Experimental data were fitted into a polynomial model to define the effects of independent variables (SC, UP, and ST) on the physicochemical and antibacterial properties of nanoemulsions using the software Statistica® 10 (StatSoft, EUA). The polynomial model used was:

$$Y = B_0 + \sum_{i=1}^{3} B_i X_i + \sum_{i=1}^{3} B_{ii} X_i^2 + \sum_{i=1}^{2} \sum_{j>i}^{3} B_{ij} X_i X_j + \varepsilon \quad (3)$$

where Y is the response observed on the dependent variable; B_0 is the regression constant; B_i, B_{ii}, and B_{ij} are the coefficients of the regression model; X_i and X_j indicate the linear effects of the independent variables; and X_i^2 refers to the quadratic effect of the independent variables, while X_{ij} refers to the impact of the interaction between the independent variables. The goodness of fit was determined with a significance level of 5% ($P < 0.05$) for independent variables, determination coefficient (R^2 and *Adj.* R^2), and lack of fit ($P \geq 0.05$). The Shapiro–Wilk test was used to verify the normality of residual data. The graphical representation of the model obtained was presented using the response surface methodology (RSM).

Model Validation and Optimization of the Nanoemulsion Process

Model validation was performed in eight additional random experiments in triplicate that did not include the conditions applied to construct the mathematical model

(Table S2/Supplementary Information). The accuracy factor (A_f) (Eq. 4) and the bias factor (B_f) (Eq. 5) were calculated according to (Baranyi et al., 1999). A_f indicates the dispersion of data about predicted values, and B_f indicates the agreement between predicted and observed values. Values of A_f and B_f close to 1.0 are considered ideal, with an acceptable variation limit of up to 0.45 for each model variable (Ross et al., 2000). After validation, the droplet diameter, PDI, zeta potential, and MIC variables were optimized to the minimum possible based on overall desirability values using the software Statistica® 10 (StatSoft, EUA).

$$A_f = exp\left(\sqrt{\frac{\sum_{k=1}^{m}\left(Lnf\left(x^{(k)}\right) - Ln\mu^{(k)}\right)^2}{m}}\right) \quad (4)$$

$$B_f = exp\left(\sqrt{\frac{\sum_{k=1}^{m}\left(Lnf\left(x^{(k)}\right) - Ln\mu^{(k)}\right)}{m}}\right) \quad (5)$$

where $Lnf\,(x)$ is the value predicted by the model, $Ln\mu$ is the observed value, and m is the number of experiments.

Optimized Nanoemulsion Stability Throughout Storage

Storage stability of *n*OEO was evaluated for 30 days at 4 °C and 25 °C. Droplet diameter, PDI, and zeta potential were determined on days 0, 10, 20, and 30 days of storage.

One-way ANOVA was performed followed by Duncan's test at 5% significance to determine differences in storage times in *n*OEO stability assays. Furthermore, a linear regression analysis was used to establish relationships between storage time and an increase in droplet size. The goodness of fit of the polynomial model was expressed by the coefficient of determination (R^2 and adjusted R^2), and the F test verified its statistical significance. These analyses were performed using the XLSTAT (2022) software.

Results and Discussion

Mathematical Model Adjustment

The effects of processing variables (SC, UP, and ST) on the physicochemical (DS, PDI, and ZP) and antibacterial (MIC) properties of the droplets are presented in Table S1 of the supplementary information. Droplet diameter ranged from 41.67 to 231.83 nm. The PDI ranged from 0.21 to 0.46; ZP was between −5.19 and −12.40 mV; and the MIC ranged from 0.11 to 1.83 mg/mL for the two pathogens evaluated.

The estimated effects for each variable and the performance indices of the mathematical model are presented in Table 2. The lack of fit values was not significant ($P \geq 0.05$), indicating that the model correctly specifies the relationship between the independent and dependent variables, considering that this term was calculated by applying the error variance independently of the model predictions (Smith & Rose, 1995). The high values obtained for the coefficients of multiple determination (R^2) and the coefficients of adjusted multiple determination ($Adj.\ R^2$) indicated that the model was efficient in adjusting the data about the real conditions of the experiment. This way, the model agreed with the predicted and observed values.

The validation performed in eight random experimental conditions within the CCRD presented an A_f and B_f range of 0.99 and 1.26. The A_f values indicate a discrepancy between predicted and observed values when values above 1.45 are found. The values of the present study are within a considerable range according to the predictive model proposed by (Baranyi et al., 1999). Values of B_f above or below 1 indicate that the model predicts values greater or less than those observed, respectively (Ross, 1996). In this case, the proposed mathematical model satisfactorily describes the effects of the nanoemulsion processing variables on the nanodroplet properties and antibacterial activity variables.

Table 2 Estimated effects for each significant variable and validation of the mathematical model ($P < 0.05$)

Variable	*DS* $_{(Y1)}$	*PDI* $_{(Y2)}$	*ZP* $_{(Y3)}$	*MIC E. coli* $_{(Y4)}$	*MIC S. aureus* $_{(Y5)}$
Intercept	97.81	0.27	−11.70	0.29	0.61
SC	−50.41	−0.10	−1.14	−0.48	−0.16
SC^2	72.72	0.07	1.38	0.74	0.64
UP	33.67	0.02	−0.39	0.22	ns
UP^2	22.66	ns	1.21	ns	−0.13
ST	44.41	ns	0.36	0.10	0.15
ST^2	ns	ns	2.45	ns	−0.23
SC × UP	ns	0.07	1.76	0.15	ns
SC × ST	44.91	ns	−1.91	0.25	0.31
UP × ST	−16.80	ns	−1.39	0.13	ns
Normality (*P* value)	0.83	0.10	0.14	0.10	0.06
Lack of fit (*P* value)	0.09	0.16	0.40	0.41	0.10
R^2	0.95	0.84	0.89	0.98	0.90
Adj R^2	0.92	0.80	0.82	0.96	0.85
A_f	1.06	1.11	1.11	1.26	1.23
B_f	0.99	1.07	1.00	1.04	1.05

SC surfactant concentration, *UP* ultrasound power, *ST* sonication time, *DS* droplet size, *PDI* polydispersity index, *ZP* zeta potential *MIC* minimum inhibitory concentration, A_f, accuracy factor, B_f, bias factor, *ns* non-significative ($P \geq 0.05$)

Evaluation of Physicochemical and Antibacterial Droplet Properties Using RSM

Droplet Size

It is possible to observe that the droplet diameter is reduced when the surfactant concentration increases and the sonication time decreases (Fig. 1a). An important surface region with droplet diameter < 100 nm is observed when the surfactant concentration is 2 to 3.5% and the sonication time is below 4 min. Several authors define nanoemulsions as having droplet diameters < 200 nm (Barradas & Silva, 2021; Zhang & McClements, 2018). Most conditions evaluated in this study follow this classification, except for extended sonication times, high ultrasound power, and low surfactant concentrations.

When observing the interaction of UP × ST, it is noticed that the lower powers in short sonication times reduce the droplet size. Regions with droplet sizes < 100 nm were obtained with powers of up to 450 W, considering the equipment and probe used in the experiment with sonication times less than 10 min. A similar effect can be observed in a study by Salvia-Trujillo et al. (2013) in which droplet sizes below 45 nm were obtained with sonication times below 180 s with a formulation based on Tween 80 and lemongrass essential oil (1 : 1 SOR). Up to a specific value, increasing the power level facilitates the breakup of the droplets, reducing the droplet diameter due to an increase in acoustic cavitation, as is observed in regions smaller than 100 nm in size. However, it is possible to observe that the droplet diameter increases with increasing power at any sonication time (Fig. 1b). The droplet diameter can increase at high powers due to the higher rate of collisions between droplets that occur in strongly turbulent shear flows in the system, favoring coalescence. Even in an ideal SOR, this effect is called "overprocessing" (Paniwnyk, 2017). This effect is observable in the present study at sonication times above 15 min at a power above 600 W, where droplet sizes are above 150 nm.

Under different conditions of ultrasound equipment, sample volume, and probe diameter, the acoustic density energy (AED) must be considered for reproducibility, as presented in Droplet Size, Polydispersity Index (PDI), and Zeta Potential. Therefore, under the conditions of sonication time and power of the optimal region, the use of AED ≥ 69.9 kJ/mL and ≤ 439.5 kJ/mL is recommended, as they represent conditions for obtaining *n*OEO ≤ 100 nm with concentrations of 2% Tween 80.

The relationship between surfactant and essential oil concentrations ratio can be a relevant factor for the final droplet diameter. The *Origanum vulgare* essential oil concentration was standardized across the study to 1%, and smaller droplets were obtained with higher SOR ratios for the surfactant up to a certain sonication time. The results of Sepahvand et al. (2021) are similar and obtained droplet sizes of approximately 86.39 nm using 2 : 1 SOR, 400 W power with 4 min of sonication for thymol. In the same line, Jiménez et al. (2018) obtained droplet sizes < 50 nm with 5 : 1 SOR in nanoemulsions of *Cinnamomum zeylanicum* and *Piper nigrum* even with 12 min of sonication with 30% amplitude (ultrasound with a maximum power of 750 W). Alternatively, Ozogul et al. (2020) obtained droplet sizes of approximately 447.60 nm using 1 : 10 SOR on *Thymus vulgaris* nanoemulsions. Surfactant is required during the emulsification process to reduce the interfacial tension of the system, and ideal concentrations must be added to adsorb onto the oil droplet. The interfacial energy and the formation

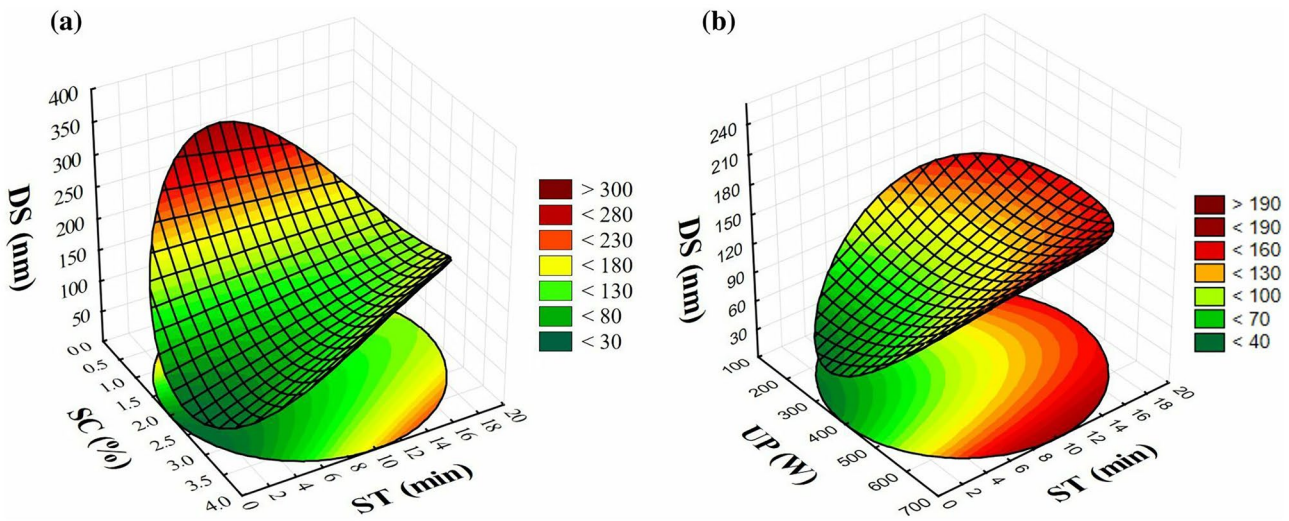

Fig. 1 3D response surface graphs of **a** SC × ST and **b** UP × ST. DS, droplet size; ST, sonication time; UP, ultrasound power

of curvature at the interface generate a pressure difference in the internal and external regions of the droplet, called Laplace pressure, which keeps the droplet stable. This pressure acts as a resistance to any attempt by applied energy to cause the droplet to rupture and fragment the droplets. It is necessary to apply a voltage equal to or greater than the Laplace pressure in the system (Gharibzahedi & Jafari, 2018). SOR of up to 3 : 1 is recommended for the conditions of the present study, as they are already sufficient to reduce the droplet size in sizes ≤ 100 nm when using low powers and sonication times.

PDI The polydispersity index determines droplet size homogeneity in an emulsion system. PDI values ≤ 0.25 indicate homogeneous droplets, and values > 0.5 are considered heterogeneous dispersion in the system (Pinelli et al., 2021). The PDI values obtained in the RSM of the present study are shown in Fig. 2. Using surfactant concentrations above 3% with powers below 200 W formed more homogeneous *n*OEO (PDI < 0.20), considering the graphic region with the lowest value. Increasing the surfactant concentration to a certain point reduces the PDI, indicating a more homogeneous dispersion of the nanodroplets. According to the mathematical model, the interaction between surfactant concentration and ultrasound power was significant ($P < 0.05$) (Table 2). However, the low estimated effect seems to have little influence on the polydispersity of the nanodroplets, as observed by the contour lines almost parallel to the ultrasound power axis.

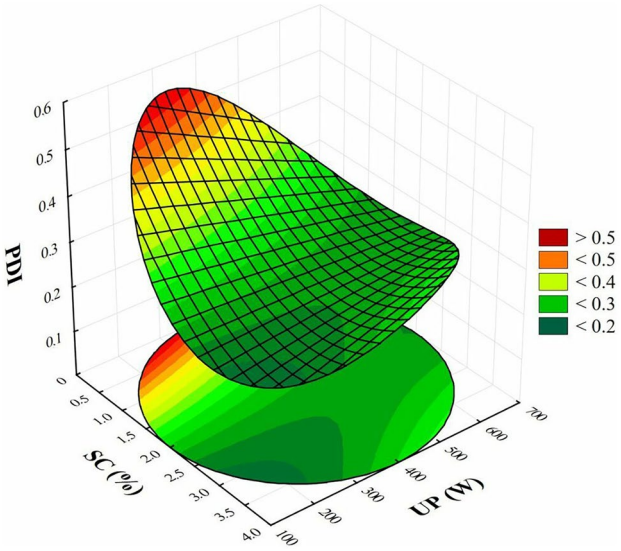

Fig. 2 3D response surface optimization graphs of SC × UP. PDI, polydispersity index; SC, surfactant concentration; UP, ultrasound power

The PDI is a complementary variable to the droplet size that helps to understand the behavior of the instability phenomena of nanoemulsions. Heterogeneous nanoemulsion systems favor droplet coalescence and Ostwald ripening, which increase droplet size over storage time. Increases in droplet heterogeneity occur when there are low concentrations of surfactant in the system, depending on certain conditions. When the surfactant is not added sufficiently to adsorb at the oil droplet interface, coalescence phenomena occur more intensely, increasing the droplet size (Ferreira & Nunes, 2019). Effects on PDI caused by the use of low concentrations of surfactant are observed in this work when the SOR was < 2 : 1.

Zeta Potential

The zeta potential was impacted by the three processing variables evaluated (Fig. 3). It is possible to observe an important region with zeta potential > −11 mV on the response surfaces when Tween 80 concentrations are between 1.0 and 3.5%. With the increase in surfactant concentration, it is necessary to reduce the ultrasound power to reach the lowest values of zeta potential in times close to 10 min. Tween 80 is a non-ionic surfactant composed of 20 units of ethylene oxide, sorbitol, and one oleic acid as primary fatty acid (Pubchem, 2022). It is suggested that these effects for the zeta potential occurred due to the fragmentation of Tween 80 when subjected to high acoustic energy density, causing the release of free fatty acids in the system and an increase in the electrical charge of the suspension.

For antibacterial activity, the electrical charge of the nanodroplets must be evaluated in a complementary way to the other physicochemical variables (droplet size and PDI) and not in isolation since droplets without electrical charge or with the same sign of surface charge bacterial cells may have better antibacterial effects than pure oil (Jiménez et al., 2018; Shokri et al., 2020). The different mechanisms of action coexist and can act when nanoemulsions are in contact with bacterial cells.

MIC The MIC obtained for OEO in the present study was 2.36 mg/mL for *E. coli* and *S. aureus* in approximate concentrations of 5.5 log CFU/mL confirmed in Mueller Hinton agar. All the conditions evaluated for the *n*OEO in the pathogens showed lower MIC values than the pure oil, with a variation between 0.15 and 1.83 mg/mL (Table S1/Supplementary Information).

The RSM of MIC to *E. coli* and *S. aureus* are shown in Fig. 4. The effects observed for the MIC are associated with the thickness of the interface with the bioactive hydrophobic core and the droplet diameter reduction. The thickness of the surfactant layer in macroemulsions is generally less

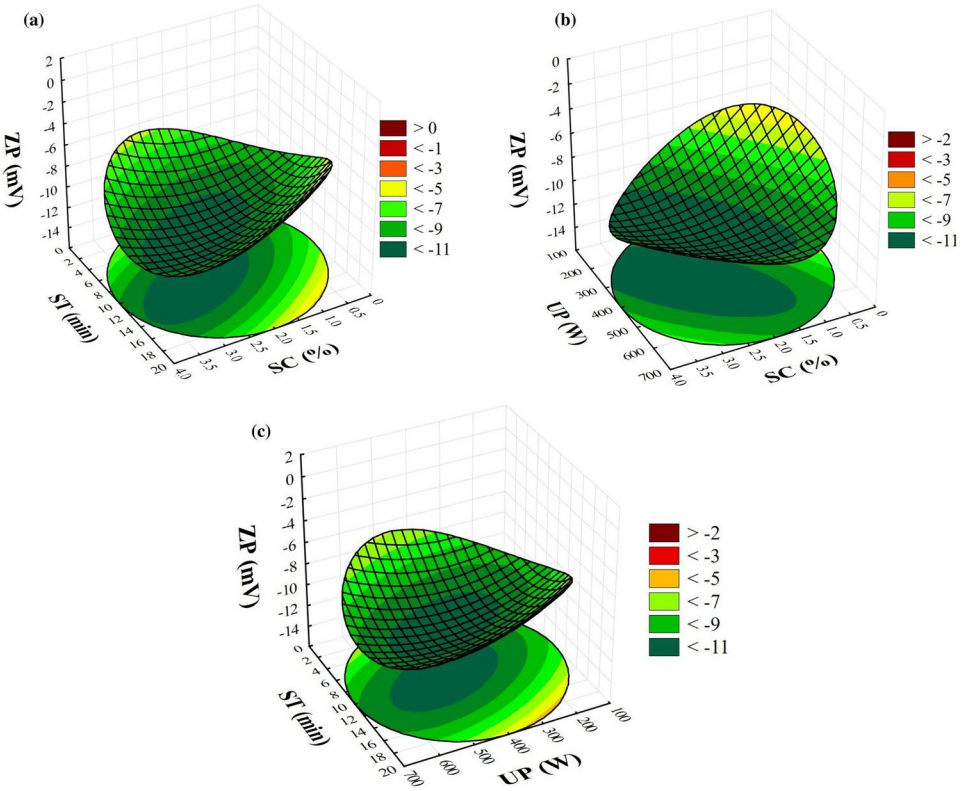

Fig. 3 3D response surface optimization graphs of **a** SC × ST, **b** SC × UP, and **c** UP × ST for zeta potential. SC, surfactant concentration; UP, ultrasound power; ST, sonication time; ZP, zeta potential

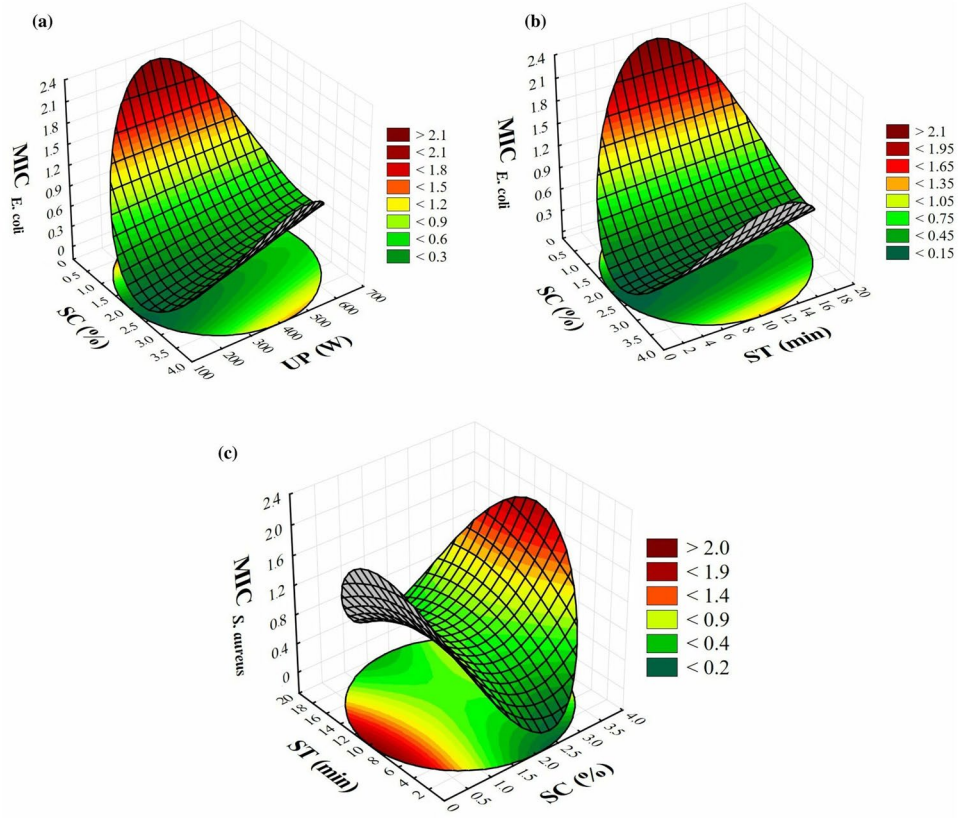

Fig. 4 3D response surface optimization graphs of **a** SC × UP for *E. coli* and **b** SC × ST for *E. coli* and **c** SC × ST for *S. aureus*. SC, surfactant concentration; UP, ultrasound power; ST, sonication time; MIC, minimum inhibitory concentration

than the radius of the hydrophobic core, with the droplets being mainly oil. However, the thickness of the surfactant layer adsorbed on nanodroplets may have dimensions similar to the hydrophobic core, directly influencing the general droplet composition, solubility, size, and bioactivity (Tadros et al., 2004).

Two types of observations can be made about the results obtained on the response surface. First, reductions of up to 8 × the inhibitory concentration of pure oil could be obtained for nanoemulsions produced with Tween 80 concentrations between 2 and 3.5% in < 4 min for *S. aureus* and < 12 min for *E. coli*. Ultrasound power values below the central point (412 W) also reduced the MIC to *E. coli*. The second observation is that at Tween 80, concentrations above 3.5% contributed to an increase in MIC in both pathogens, which is proposed by the decrease in the bioactive hydrophobic core composed of *Origanum vulgare* essential oil. Concentrations below 2% also increased the MIC, mainly suggested by the reduction of the hydrophilic interfacial layer provided by the surfactant and the increase in droplet size (McClements et al., 2021; Ozogul et al., 2020).

The reduction of MIC values for nanoemulsions indicates that the droplet size reduction process can improve antibacterial activity. It is proposed that the observed effects are related to the physicochemical characteristics of the droplets, such as size, increase in specific surface area, and hydrophilicity of the interface. The physicochemical characteristics of the nanodroplet allow greater contact with bacterial cells present in the aqueous phase of the system, facilitating the fusion of the interfacial layer of the surfactant with the release of essential oil in the phospholipid bilayer of the membrane (Sepahvand et al., 2021). Furthermore, no critical difference in antibacterial effect was observed due to the cellular structure of the present study between *E. coli* and *S. aureus*. The differences in effect observed in studies with pure oil between Gram-negative and Gram-positive are less observed in nanodroplets (Badr et al., 2021; Enayatifard et al., 2021). This is because the droplet size facilitates the exposure of hydrophilic groups of Tween 80 that can be easily transported through porins of the outer membrane of Gram-negative bacteria, making the essential oil delivery system capable of fusing with the cytoplasmic membrane (Nazzaro et al., 2013).

Optimization of Nanoemulsion Properties

According to the mathematical model, the droplet diameter, PDI, zeta potential, and MIC variables for *E. coli* and *S. aureus* were optimized based on general desirability as an evaluation index. The predicted optimal conditions (92.20% desirability) were 2.9% of Tween 80, 157 W of ultrasound power, and 4.7 min of sonication to obtain the approximate values of the variables of nanodroplet properties and antibacterial activity (DS = 41 nm ± 27 nm (IC); PDI = 0.21; ZP = −10,13 mV; $MIC_{pathogens} = \leq 0.23$ mg/mL). In ultrasound with power ranges and probe diameters different from those used in the present study, the authors recommend applying an AED of approximately 81.4 kJ/mL + 2.9% Tween 80, equivalent to the optimized condition obtained. In a previous meta-analysis study, it was possible to observe the antibacterial behavior of nanoemulsions in several ultrasound studies (da Silva et al., 2022b). When the concentration of surfactant used in processing was slightly higher (SOR ~ 3 : 1), the droplets generated mostly had improved antibacterial properties compared to the free versions. This information corroborates the conditions optimized in the present study.

Optimized Nanoemulsion Stability Throughout Storage

The physicochemical properties of *n*OEO optimized during storage are shown in Table 3. Notably, all physicochemical properties obtained after preparing the optimized *n*OEO were close to those estimated by the desirability model within the 95% confidence interval. Polydispersity and zeta potential of nanodroplets did not show significant differences during storage at 4 °C. Nanoemulsions stored at 25 °C showed no significant change in zeta potential ($P \geq 0.05$). However, the PDI increased significantly during the 30 days ($P < 0.05$). Polydispersion indices of the optimized

Table 3 Stability of *n*OEO during storage at 4 °C and 25 °C

		0 days	10 days	20 days	30 days
4 °C	DS (nm)	54.30 ± 1.28^{4}	80.77 ± 5.12^{3}	100.73 ± 1.56^{2}	135.74 ± 16.07^{1}
	PDI	0.18 ± 0.06	0.18 ± 0.03	0.17 ± 0.02	0.16 ± 0.03
	ζ (mV)	−10.91 ± 1.46	−11.90 ± 0.56	−11.36 ± 0.85	−10.90 ± 1.07
25 °C	DS	54.30 ± 1.28^{4}	154.86 ± 6.56^{3}	244.82 ± 29.53^{2}	373.87 ± 33.22^{1}
	PDI	0.18 ± 0.06^{2}	$0.25 \pm 0.02^{1,2}$	0.30 ± 0.03^{1}	0.32 ± 0.03^{1}
	ζ (mV)	−10.91 ± 1.46	−12.80 ± 1.34	−13.20 ± 0.94	−13.04 ± 1.94

DS droplet size, *PDI* polydispersity index, (ζ) zeta potential. Different lowercase letters on the same line indicate significant differences according to Duncan's test ($P < 0.05$)

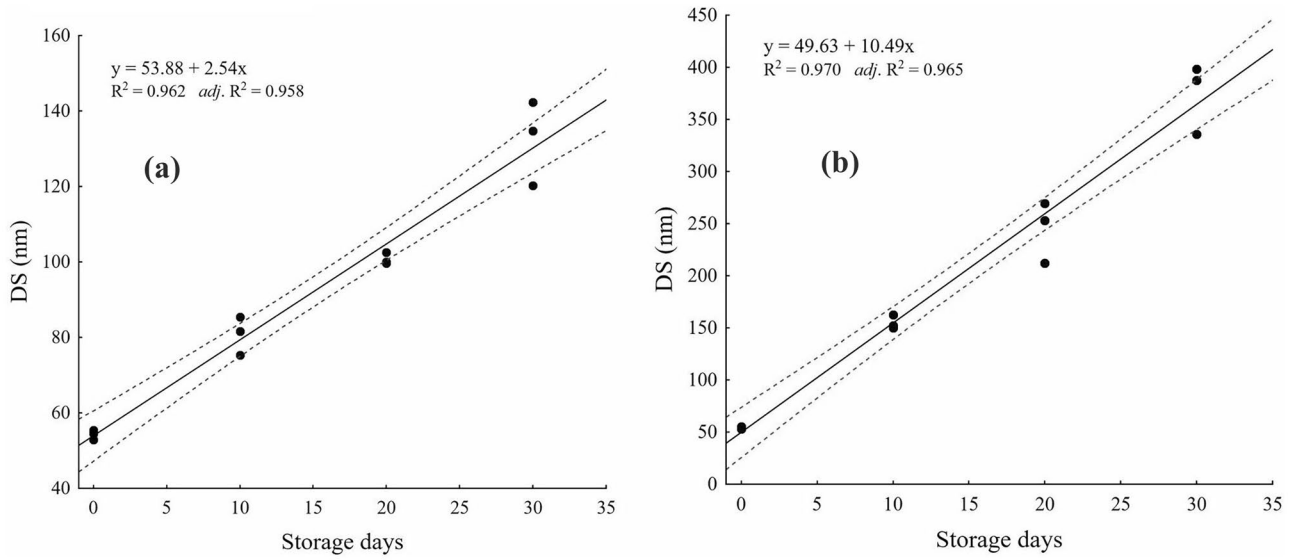

Fig. 5 Kinetics of growth of nanodroplets during storage at 4 °C (**a**) and 25 °C (**b**). DS, droplet size

nanoemulsions were below 0.25, indicating monodispersity in droplet size. For the zeta potential, the values of the present study were between −12.01 and −13.20 mV during storage.

During the entire storage period at 4 °C, the nanoemulsions had droplet diameters smaller than 150 nm. In storage at 25 °C, there was an expressive and significant increase throughout storage, with droplets exceeding 200 nm in the first 20 days ($P < 0.05$).

It is essential to distinguish thermodynamic stability from kinetic stability. While thermodynamic stability will tell you whether or not a process will occur (no matter how long it takes to complete it), kinetics will tell you the rate (timescale) and degree of change when it occurs (Silva et al., 2015). Nanoemulsions are thermodynamically unstable due to unfavorable molecular interactions at the oil–water interface, generating a thermodynamic driving force to reduce the contact area between the hydrophobic and hydrophilic phases. Consequently, nanoemulsions always tend towards phase separation over time. The time for phase separation is controlled by the kinetic energy of the droplets in the system, and nanoemulsions are considered kinetically stable under the influence of Brownian motion (McClements & Jafari, 2018). Particles smaller than 100 nm have kinetics predominantly influenced by Brownian motion, reducing the impacts of instability phenomena (da Silva et al., 2022a).

In the present study, the droplet size growth kinetics represented a daily increase of 2.67 nm, with an approximate total accumulation of 80.10 nm during the entire storage at 4 °C (Fig. 5a). When subjected to a temperature of 25 °C, the daily growth kinetics of the droplets increased to 10.56 nm (Fig. 5b). In a study by Teng et al. (2020), the size of phosphatidylcholine nanoemulsions increased with the change in temperature from 4 to 25 °C, due to the increase in kinetic energy and, consequently, the Brownian motion, which increased the frequency of collisions between the drops. Alternatively, Hasheminya and Dehghannya (2022) did not observe a significant increase in nanodroplet size (< 100 nm) of *Froriepia subpinnata* essential oil in the first 45 days of storage at 25 °C. This difference in size increase over time can be attributed to the electrical charge of the droplets. In the studies cited above, the zeta potential of the droplets was less than −30 mV, and in the present study, they were higher than −13 mV (Hasheminya & Dehghannya, 2022; Teng et al., 2020). This difference may favor coalescence between nanodroplets in systems with higher temperatures due to higher kinetic energy between molecules and lower electrostatic repulsion.

Conclusion

The concentration of Tween 80 was essential for the preparation of the nanoemulsions, being the only processing variable that was present in the significant interactions ($P < 0.05$) of all the observed properties of the nanodroplets and antibacterial activity. The addition of surfactant at concentrations higher than the essential oil, with acoustic cavitation for short periods at low power, formed homogeneous nanoemulsions with droplet diameters smaller than 100 nm. In addition, under all conditions evaluated, the antibacterial properties were better than pure *Origanum*

vulgare oil. The optimal conditions predicted by the model were 2.9% Tween 80, 157 W of ultrasound power, and 4.7 min of sonication to obtain the best droplet properties and antibacterial activity. In addition, the optimized nanoemulsions showed considerable stability over 30 days of refrigerated storage, remaining below 150 nm. Under different process conditions (equipment, probe diameter, and sample volume), we recommend using acoustic energy density to approximate the conditions of the present study.

It is worth mentioning that in different process conditions (equipment, probe diameter, and sample volume), the acoustic density energy is the most recommended to approach the conditions of the present study. The chemical composition of the oil can also vary depending on the regions of cultivation, climatic conditions, and extraction and storage methods. However, it is believed that even with variations in chemical composition, it is possible to obtain essential oil nanoemulsions with improved physicochemical and antibacterial properties compared to pure oil.

Supplementary Information The online version contains supplementary material available at https://doi.org/10.1007/s11947-023-03050-z.

Author Contribution Bruno Dutra da Silva: Conceptualization, Investigation, Formal analysis, Writing-original draft, Writing-review, and Editing; Denes Kaic Alves do Rosário: Conceptualization, Project administration, Supervision, Writing-Review, and Editing; Yago Alves de Aguiar Bernardo: Investigation, Formal analysis, Writing-Review, and Editing; Carlos Adam Conte-Junior: Project administration, Supervision, Funding acquisition, Writing-Review, and Editing. All authors have read and agreed to the published version of the manuscript.

Funding The authors are thankful for the financial support provided by the Fundação Carlos Chagas de Amparo à Pesquisa do Estado do Rio de Janeiro (FAPERJ) Brazil — grant number [E-26/203.049/2017 and E-26/010.000.984/2019], the Fundação de Amparo à Pesquisa e Inovação do Espírito Santo (FAPES)/PDCTR grant number [533/2020], the Conselho Nacional de Desenvolvimento Científico e Tecnológico (CNPq)—grant number [140873/2021–0], and the Coordenação de Aperfeiçoamento de Pessoal de Nível Superior (CAPES) Brazil – Finance Code 001.

Data Availability The authors included in the present paper and its supplementary information files all the relevant data.

Declarations

Conflict of Interest The authors declare no competing interests.

References

Araújo, M. K., Gumiela, A. M., Bordin, K., Luciano, F. B., & de Macedo, R. E. F. (2018). Combination of garlic essential oil, allyl isothiocyanate, and nisin Z as bio-preservatives in fresh sausage. *Meat Science*, *143*, 177–183. https://doi.org/10.1016/j.meatsci.2018.05.002

Badr, M. M., Badawy, M. E. I. I., & Taktak, N. E. M. M. (2021). Characterization, antimicrobial activity, and antioxidant activity of the nanoemulsions of *Lavandula spica* essential oil and its main monoterpenes. *Journal of Drug Delivery Science and Technology*, *65*, 102732. https://doi.org/10.1016/j.jddst.2021.102732

Baranyi, J., Pin, C., & Ross, T. (1999). Validating and comparing predictive models. *International Journal of Food Microbiology, 48*(3), 159–166. https://doi.org/10.1016/S0168-1605(99)00035-5

Barradas, T. N., de Silva, K. G., & H. K. (2021). Nanoemulsions of essential oils to improve solubility, stability and permeability: A review. *Environmental Chemistry Letters, 19*(2), 1153–1171. https://doi.org/10.1007/s10311-020-01142-2

Bernardo, Y. A. de A., do Rosario, D. K. A., & Conte-Junior, C. A. (2021). Ultrasound on milk decontamination: Potential and limitations against foodborne pathogens and spoilage bacteria. https://doi.org/10.1080/87559129.2021.1906696

CLSI. (2006). Performance standards for antimicrobial susceptibility testing. In *Clinical and Laboratory Standards Institute document M100-S16CLSI*. Wayne, PA.

da Silva, B. D., do Rosário, D. K. A., Weitz, D. A., & Conte-Junior, C. A. (2022a). Essential oil nanoemulsions: Properties, development, and application in meat and meat products. *Trends in Food Science & Technology, 121*, 1–13. https://doi.org/10.1016/J.TIFS.2022.01.026

da Silva, B. D., Rosario, D. K. A., & Conte-Junior, C. A. (2022b). Can droplet size influence antibacterial activity in ultrasound-prepared essential oil nanoemulsions? *Critical Reviews in Food Science and Nutrition*, 1–11. https://doi.org/10.1080/10408398.2022.2103089

Donsi, F., Ferrari, G., Donsì, F., & Ferrari, G. (2016). Essential oil nanoemulsions as antimicrobial agents in food. *Journal of Biotechnology, 233*, 106–120. https://doi.org/10.1016/j.jbiotec.2016.07.005

Enayatifard, R., Akbari, J., Babaei, A., Rostamkalaei, S. S., Hashemi, S. M. H., & Habibi, E. (2021). Anti-microbial potential of nanoemulsion form of essential oil obtained from aerial parts of *Origanum vulgare* L. as food additive. *Advanced Pharmaceutical Bulletin*, *11*(2), 327–334. https://doi.org/10.34172/apb.2021.028

Ferreira, C. D., & Nunes, I. L. (2019, January 7). Oil nanoencapsulation: development, application, and incorporation into the food market. *Nanoscale Research Letters*. Springer New York LLC. https://doi.org/10.1186/s11671-018-2829-2

Galvão, K. C. S., Vicente, A. A., & Sobral, P. J. A. (2018). Development, characterization, and stability of O/W pepper nanoemulsions produced by high-pressure homogenization. *Food and Bioprocess Technology, 11*(2), 355–367. https://doi.org/10.1007/S11947-017-2016-Y/TABLES/5

Gharibzahedi, S. M. T., & Jafari, S. M. (2018). Fabrication of nanoemulsions by ultrasonication. *Nanoemulsions: Formulation, Applications, and Characterization*, 233–285. https://doi.org/10.1016/B978-0-12-811838-2.00009-6

Hasheminya, S. M., & Dehghannya, J. (2022). Development and characterization of *Froriepia subpinnata* (Ledeb.) Baill essential oil and its nanoemulsion using ultrasound. *Food and Bioprocess Technology*, *15*(11), 2531–2546. https://doi.org/10.1007/S11947-022-02899-W/TABLES/3

Hien, L. T. M., & Dao, D. T. A. (2021). Black pepper essential oil nanoemulsions formulation using EPI and PIT methods. *Journal of Food Processing and Preservation*, *45*(3), e15216. https://doi.org/10.1111/JFPP.15216

Jiménez, M., Domínguez, J. A. A., Pascual-Pineda, L. A. A., Azuara, E., Beristain, C. I. I., Jimenez, M., et al. (2018). Elaboration and characterization of O/W cinnamon (*Cinnamomum zeylanicum*) and black pepper (*Piper nigrum*) emulsions. *Food Hydrocolloids, 77*, 902–910. https://doi.org/10.1016/j.foodhyd.2017.11.037

McClements, D. J., Das, A. K., Dhar, P., Nanda, P. K., & Chatterjee, N. (2021). Nanoemulsion-based technologies for delivering natural plant-based antimicrobials in foods. *Frontiers in Sustainable Food Systems*. Frontiers Media S.A. https://doi.org/10.3389/fsufs.2021.643208

McClements, D. J., & Jafari, S. M. (2018). General aspects of nanoemulsions and their formulation. *Nanoemulsions: Formulation, Applications, and Characterization*, 3–20. https://doi.org/10.1016/B978-0-12-811838-2.00001-1

Merghni, A., Lassoued, M. A., Voahangy Rasoanirina, B. N., Moumni, S., & Mastouri, M. (2022). Characterization of turpentine nanoemulsion and assessment of its antibiofilm potential against methicillin-resistant *Staphylococcus aureus*. *Microbial Pathogenesis*, *166*, 105530. https://doi.org/10.1016/J.MICPATH.2022.105530

Nazzaro, F., Fratianni, F., de Martino, L., Coppola, R., & de Feo, V. (2013). Effect of essential oils on pathogenic bacteria. *Pharmaceuticals, 6*(12), 1451–1474. https://doi.org/10.3390/ph6121451

Ojha, K. S., Tiwari, B. K., & O'Donnell, C. P. (2018). Effect of ultrasound technology on food and nutritional quality. *Advances in Food and Nutrition Research, 84*, 207–240. https://doi.org/10.1016/BS.AFNR.2018.01.001

Ozogul, Y., Kuley Boğa, E., Akyol, I., Durmus, M., Ucar, Y., Regenstein, J. M., & Köşker, A. R. (2020). Antimicrobial activity of thyme essential oil nanoemulsions on spoilage bacteria of fish and food-borne pathogens. *Food Bioscience*, 100635. https://doi.org/10.1016/j.fbio.2020.100635

Paniwnyk, L. (2017). Applications of ultrasound in processing of liquid foods: A review. *Ultrasonics Sonochemistry, 38*, 794–806. https://doi.org/10.1016/J.ULTSONCH.2016.12.025

Pinelli, J. J., Martins, H. H. de A., Guimarães, A. S., Isidoro, S. R., Gonçalves, M. C., Junqueira de Moraes, T. S., et al. (2021). Essential oil nanoemulsions for the control of *Clostridium sporogenes* in cooked meat product: An alternative? *LWT*, *143*, 111123. https://doi.org/10.1016/j.lwt.2021.111123

Pubchem. (2022). Polyethylene oxide sorbitan mono-oleate | C32H60O10 - PubChem. https://pubchem.ncbi.nlm.nih.gov/compound/86289060. Accessed 26 August 2022

Rosario, D. K. A., Rodrigues, B. L., Bernardes, P. C., & Conte-Junior, C. A. (2020). Principles and applications of non-thermal technologies and alternative chemical compounds in meat and fish. *Critical Reviews in Food Science and Nutrition, 61*(7), 1163–1183. https://doi.org/10.1080/10408398.2020.1754755

Ross, T. (1996). Indices for performance evaluation of predictive models in food microbiology. *Journal of Applied Bacteriology, 81*(5), 501–508. https://doi.org/10.1111/J.1365-2672.1996.TB03539.X

Ross, T., Dalgaard, P., & Tienungoon, S. (2000). Predictive modelling of the growth and survival of *Listeria* in fishery products. *International Journal of Food Microbiology, 62*(3), 231–245. https://doi.org/10.1016/S0168-1605(00)00340-8

Salvia-Trujillo, L., Rojas-Graü, A., Soliva-Fortuny, R., & Martín-Belloso, O. (2013). Physicochemical characterization of lemongrass essential oil-alginate nanoemulsions: Effect of ultrasound processing parameters. *Food and Bioprocess Technology, 6*(9), 2439–2446. https://doi.org/10.1007/S11947-012-0881-Y/FIGURES/8

Sepahvand, S., Amiri, S., Radi, M., & Akhavan, H. R. (2021). Antimicrobial activity of thymol and thymol-nanoemulsion against three food-borne pathogens inoculated in a sausage model. *Food and Bioprocess Technology, 14*(10), 1936–1945. https://doi.org/10.1007/S11947-021-02689-W

Sharma, K., Babaei, A., Oberoi, K., Aayush, K., Sharma, R., & Sharma, S. (2022). Essential oil nanoemulsion edible coating in food industry: A review. *Food and Bioprocess Technology, 15*(11), 2375–2395. https://doi.org/10.1007/S11947-022-02811-6

Shokri, S., Parastouei, K., Taghdir, M., & Abbaszadeh, S. (2020). Application an edible active coating based on chitosan- *Ferulago angulata* essential oil nanoemulsion to shelf life extension of rainbow trout fillets stored at 4 °C. *International Journal of Biological Macromolecules, 153*, 846–854. https://doi.org/10.1016/j.ijbiomac.2020.03.080

Silva, H. D., Cerqueira, M. A., & Vicente, A. A. (2015). Influence of surfactant and processing conditions in the stability of oil-in-water nanoemulsions. *Journal of Food Engineering, 167*, 89–98. https://doi.org/10.1016/J.JFOODENG.2015.07.037

Smith, E. P., & Rose, K. A. (1995). Model goodness-of-fit analysis using regression and related techniques. *Ecological Modelling, 77*(1), 49–64. https://doi.org/10.1016/0304-3800(93)E0074-D

Tadros, T., Izquierdo, P., Esquena, J., & Solans, C. (2004). Formation and stability of nano-emulsions. *Advances in Colloid and Interface Science, 108–109*, 303–318. https://doi.org/10.1016/J.CIS.2003.10.023

Teng, F., He, M., Xu, J., Chen, F., Wu, C., Wang, Z., & Li, Y. (2020). Effect of ultrasonication on the stability and storage of a soy protein isolate-phosphatidylcholine nanoemulsions. *Scientific Reports, 10*(1), 1–9. https://doi.org/10.1038/s41598-020-70462-8

Wiegand, I., Hilpert, K., & Hancock, R. E. W. (2008). Agar and broth dilution methods to determine the minimal inhibitory concentration (MIC) of antimicrobial substances. *Nature Protocols, 3*(2), 163–175. https://doi.org/10.1038/nprot.2007.521

Xu, J., Zhou, L., Miao, J., Yu, W., Zou, L., Zhou, W., et al. (2020). Effect of cinnamon essential oil nanoemulsion combined with ascorbic acid on enzymatic browning of cloudy apple juice. *Food and Bioprocess Technology, 13*(5), 860–870. https://doi.org/10.1007/S11947-020-02443-8/FIGURES/6

Youssef, A. M., El-Sayed, H. S., El-Sayed, S. M., Fouly, M., & El-Aziz, M. E. A. (2022). Novel bionanocomposites based on cinnamon nanoemulsion and TiO2-NPs for preserving fresh chicken breast fillets. *Food and Bioprocess Technology, 16*(2), 356–367. https://doi.org/10.1007/S11947-022-02934-W/FIGURES/6

Zhang, Z., & McClements, D. J. (2018). Overview of nanoemulsion properties: Stability, rheology, and appearance. *Nanoemulsions: Formulation, Applications, and Characterization*, 21–49. https://doi.org/10.1016/B978-0-12-811838-2.00002-3